Effect of *Bacillus* and *Pseudomonas* biofilms on the corrosion behavior of AISI 304 stainless steel

Hafiz Zeshan Wadood[1,2], Aruliah Rajasekar[2,3], Ameeq Farooq[4], Kashif Mairaj Deen[5,*]

[1]*Department of Biology, Lahore Garrison Univesity, Lahore, Pakistan*

[2]*Department of Chemical and Biomolecular Engineering, National University of Singapore, Singapore – 117576*

[3]*Department of Biotechnology, Thiruvalluvar University, Serkkadu, Vellore, India – 632 115*

[4]*Corrosion Control Research Cell, Institute of Metallurgy and Materials Engineering, CEET, University of the Punjab, Lahore, 54590, Pakistan*

[5]*Department of Materials Engineering, The University of British Columbia, Vancouver, V6T 1Z4, BC, Canada*

***Corresponding author:** kashifmairaj.deen@ubc.ca*

Abstract

In this research work, the corrosion tendency of stainless steel (SS 304) caused by the *Pseudomonas aeruginosa* ZK (PA-ZK) and *Bacillus subtilis* S1X (BS-S1X) bacterial strains is investigated. The topographical features of the biofilms and SS304 substrate achieved after 14 days of incubation at 37 °C were examined by scanning electron microscopy (SEM). Fourier Transform Infrared Spectroscopic (FTIR) analysis of the extracellular polymer substance (EPS) was also carried out to estimate the chemical composition of the biofilm. Electrochemical Impedance Spectroscopy (EIS) and Tafel Polarization test methods were applied to understand the in-situ corrosion tendency of the SS304 in the presence of PA-ZK and BS-S1X strains. Compared to the biofilm produced by the PA-ZK, the EPS in the BS-S1X containing bacteria was porous and non-uniform as revealed in the SEM analysis. The improved hydrophobicity and uniformity of the PA-ZK containing biofilm retarded the corrosion of the underlying SS304 sample. Appreciably large resistance of the PA-ZK biofilm (~ 6.04 kΩ-cm^2) and hindered charge transport (11.12 kΩ-cm^2) were evident from the EIS analysis. In support of these results, a large cathodic Tafel slope (0.2 V/decade) and low corrosion rate (1.69 μA/cm^2) were corroborated by the inhibitive properties of the PA-ZK containing biofilm. However, the formation of porous biofilm and non-homogeneity of the EPS layer produced by the BS-S1X bacteria facilitated localized corrosion. Also, low charge transfer resistance, a high corrosion rate and pitting of the surface under BS-S1X biofilm were

comparable to the surface features of SS304 obtained after exposure to a controlled medium. These results highlighted the poor corrosion inhibitive properties of the BS-S1X biofilm compared to the PK-ZK bacterial strain.
Keyword: Biofilm; Biocorrosion; *Bacterial strains*; Localized dissolution

1. Introduction

The metabolic activities of microbes on the metallic surfaces could deteriorate the structural integrity and functionality of the industrial equipment. For instance, due to the microbial activities, the origin of distinct microenvironments on the surface of the metallic structures could facilitate localized concentration, aeration and pH variations leading to localized corrosion. This dissolution of metallic materials in the presence of microbes i.e. bacteria is generally termed as microbiologically influenced corrosion (MIC) or biocorrosion [1-3]. MIC of any metal/alloy is a complex process and the extent of deterioration depends on many factors i.e. the nature of microbes, surface topography, alloying additions, microstructural features, aerobic/anaerobic environment etc. A noticeable impact of the MIC has been experienced by medical equipment, bioimplants, transmission oil and gas pipelines, storage tanks, power generation units, fuel tanks, aircraft, and structures exposed to the marine environment [4, 5]. Stainless steel (SS304) is a common alloy and is widely used in many industrial applications due to its adequate mechanical and corrosion-resistant properties. The SS304 is the best-known corrosion-resistant alloy due to its tendency to form thin, adherent, and protective passive film under oxidizing conditions [6]. MIC is usually interpreted as the process which is associated with the accelerated dissolution of metallic surface underlying extracellular polymeric substance (EPS) layer containing biofilm produced by the biological activity of the bacteria strain [2]. On the other hand, some microbes are considered beneficial to inhibit corrosion in natural environments due to the barrier characteristics of the biofilms and their tendency to avoid cathodic depolarization [7-9]. Mostly, due to the corrosion process, the dissolved ionic species could disturb the barrier characteristics of the EPS and the MIC is accelerated in the presence of microbial biofilms [10-13]. Microbiologically influenced corrosion inhibition (MICI) is important and is promoted by two types of mechanisms. In the first mechanism, corrosion inhibiting microbes can inactivate the corrosion causing microbes through metabolic activities. During their metabolism, they can either consume oxygen from the surrounding environment by varying the pH of the EPS, which can affect the biological

activity of the aggressive bacteria. Secondly, the inhibiting microbes can restrict the corrosion of metallic surfaces by forming protective biofilms on the surface [14, 15].

The purpose of this research is to understand the corrosion behavior of biofilms formed by *Pseudomonas aeruginosa* ZK (PA-ZK) and *Bacillus subtilis* S1X (BS-S1X) in the highly saline environment on the surface of the AISI304 stainless steel (SS304). The in-situ corrosion behavior of stainless steel was investigated in both the controlled and inoculated media incubated for 14 days at 37 °C with the help of electrochemical impedance spectroscopy (EIS) and Tafel polarization method. The surface morphology and composition of the biofilm formed on the surface of SS304 were examined by SEM and FTIR analysis.

2. Experimental

Hydrophobicity characterization of bacterial strains

The bacterial strains namely *Pseudomonas aeruginosa* ZK and *Bacillus subtilis* S1X were isolated and cultured in the minimal salt medium (MSM) by following the procedure as described elsewhere [16, 17]. To determine the hydrophobicity of these bacterial strains, bacterial adhesion to hydrocarbons (BATH) and salt aggregation (SA) tests were conducted by following the test protocols as described elsewhere [18, 19]. All the tests were conducted in triplicate to ensure reproducibility. Briefly, during the BATH test, the bacterial cultures were centrifuged at 5500 rpm overnight at a constant temperature of 4 °C. The supernatant was discarded and the pellet was resuspended in phosphate/urea/Mg (PUM) buffer solution after washing two times with the same buffer solution. The optical density (OD) of the suspension was determined at 600nm and set to 1.0 (A_0) by using a spectrophotometer (*Shimadzu UV-Vis*). This suspension (500 ml) was vortexed with 500 µl of hexadecane and the mixture was allowed to separate for 10-15 minutes. In this mixture, the optical density of the aqueous phase (A_1) was measured at 600 nm and the degree of hydrophobicity (D_h) was calculated by using equation 1.

$$D_h = 1-[(A_1/A_0)] \times 100\ (\%) \qquad .1$$

During the SA test, the bacterial culture was incubated and spun at a 5500 rpm rotation rate for 24 hours at 4 °C. The obtained pellet was washed (twice) and resuspended in 0.002 M sodium phosphate buffer having pH 6.8. A 4 M solution of ammonium sulphate [$(NH_4)_2SO_4$] was diluted using sodium phosphate buffer solution according to the scheme given in table 1.

Table 1: Detail of ammonium sulphate dilution used for SA test

Sets of dilution	Range of dilutions	Difference per dilution
Set 1	4 M to 0.2 M	0.2 M
Set 2	0.2 M to 0.02 M	0.02 M

The bacterial suspension was mixed with each dilution in 24 well tissue culture plates and was gently shaken for uniform mixing. The culture plate was visualized for any aggregation against a dark-colored background. The extent of hydrophobicity was qualitatively characterized by observing the aggregation patterns i.e. highly hydrophobic (aggregation < 0.1M), hydrophobic aggregation 0.1 – 1M and aggregation >1M is considered as hydrophilic.

Preparation of AISI 304 stainless steel samples

The AISI 304 stainless steel (SS304) sheet was purchased from *Nippon Yakin Kogyo Co. Ltd. Japan.* The chemical composition of SS304 is given in Table 2. Disc-shaped samples of two different diameters such as 10 mm and 14 mm were cut from the SS304 sheet having a thickness of 2 mm. These disc samples were sequentially ground on SiC paper from 240 to 1200 grit size and polished on a polishing cloth impregnated with 1 μm diamond suspension.

Table 2: Chemical composition of AISI 304 stainless steel sample

Elements	C	Cr	Ni	Cu	N	Mn	Mo	P	S	Si	Fe
Wt. %	0.053	18.08	8.18	0.06	0.047	1.68	0.05	0.037	0.007	0.43	Balance

Estimation of SS304 surface damage in the presence of bacterial strains

The biocorrosion behavior of the SS304 disc samples was determined in a controlled medium and media containing two different bacterial strains. For instance, 0.5 litres sterile MSM was used as a controlled medium designated as system 1 (S1). System 2 (S2) and 3 (S3) were composed of inoculum of 2.5 ml (0.5 %) of each *P. aeruginosa* strain ZK and *B. subtilis* strains, respectively seeded in the MSM (S1). For instance, in S2 and S3 media, the initial bacterial dose of 6.3×10^6 cfu/ml (*P. aeruginosa* ZK) and 8.4×10^3 cfu/ml (*B. Subtilis* S1X) was added in the S1 medium. In these media, sodium chloride 3% (w/v) was also added as a background solution. The SS304 disc samples were immersed in these media separately and incubated at 37 °C for two weeks. Post-surface characterization of the disc samples was carried out to examine the extent of surface damage caused by the bacterial strains. Briefly, to study the compactness of biofilms formed on the surface of SS304 samples, the biofilms were fixed on the surface using 3 % glutaraldehyde. To estimate the corrosion damage of the SS304 samples specifically caused by the bacteria in the

biofilm, the disc samples were removed after exposure to S1, S2 and S2 media and were cleaned by immersing in 1 M HNO_3 solution for 15 minutes at 60 ℃. After the removal of biofilm, the surface morphology of the SS304 samples was examined in the scanning electron microscope (*SEM: JEOL JSM-5600*). The chemical composition of the SS304 surface after biofilm removal was determined by using Fourier Transform Infrared (FTIR) spectroscopy (*Bio-Rad FTS-3500 ARX*), operated in the infrared-reflectance mode. The FTIR spectra were obtained within 400 – 4,000 cm^{-1} wavenumbers with 8 cm^{-1} resolution at a scan rate of 64 scans per spectrum.

The corrosion tendency of the SS304 disc samples was also evaluated in the S1, S2 and S3 media individually by electrochemical impedance spectroscopy and Tafel polarization tests conducted at a constant temperature of 37 ℃ after 14 days of incubation. In the three-electrode electrochemical cell, the SS304 disc samples were connected to the working/working sense lead of the cell cable connected with the Gamry Potentiostat (Interface 1000). In this cell, a Pt wire and Ag/AgCl electrodes were used as auxiliary and reference (0.199 V vs. SHE) electrodes, respectively.

3. Results

The hydrophobicity of the surface towards bacteria was estimated by BATH and salt aggregation (SA) tests. Both bacterial strains were found to be hydrophobic. The degree of hydrophobicity values (in %) of the bacterial strains are calculated by the BATH test as given in Table 3. Both PA-ZK (36.6%) and BS-S1X (35.5%) strains presented almost similar degrees of hydrophobicity on the SS304 surface. On the other hand, the SA test results showed aggregation of bacterial cells with all concentrations of $(NH_4)_2 SO_4$ (from 0.02 M to 4.0 M).

Table 3: Bacterial Adhesion to hydrocarbons BATH Test results

Bacterial strains	**Degree of hydrophobicity (%)**
***Bacillus subtilis* strain S1X**	35.5
***Pseudomonas aeruginosa* strain ZK**	36.6

Figure 1a shows the Nyquist plots of the SS304 samples immersed in each S1, S2, and S3 media. These impedance plots were simulated to an equivalent electric circuit (EEC) model by fitting the experimental spectra. In this EEC model, the properties of biofilm, i.e., charge relaxation and transport through the biofilm are represented as constant phase element (Y_{bf}) and biofilm resistance (R_{bf}), respectively (**Figure 1b**). On the other hand, the dissolution behavior of SS304 was associated with the parallel electrochemical processes i.e., the non-uniform charge distribution in

the double and progress of faradaic processes at the biofilm/substrate interface as represented by Y_{dl} and R_{ct} parameters, respectively. The 'R_s' represents the solution resistance and depends on the ionic conductivity of the S1, S2, and S3 media. The systems inoculated with bacterial strains showed a large R_{bf} and R_{ct} values compared to the values obtained in the controlled medium (S1) (Table 4). The relatively small R_{bf} and R_{ct} values of SS304 in the S1 medium compared to S2 and S3 media corresponded to the aggressiveness MSM medium. However, in the presence of bacterial strains, the larger values of R_{ct} were attributed to the formation of biofilm that hindered the approach of electrolyte to the biofilm/substrate interface. In other words, this behavior is related to the barrier characteristics of the biofilm and restricted the transport of ionic species to the interface as evident from the relatively large values of R_{bf}. Approximately 1.5 times larger R_{bf} and ~2 times lower Y_{bf} of *Bacillus subtilis* strain compared to the *Pseudomonas aeruginosa* strain was associated with the intrinsic behavior of the biofilm.

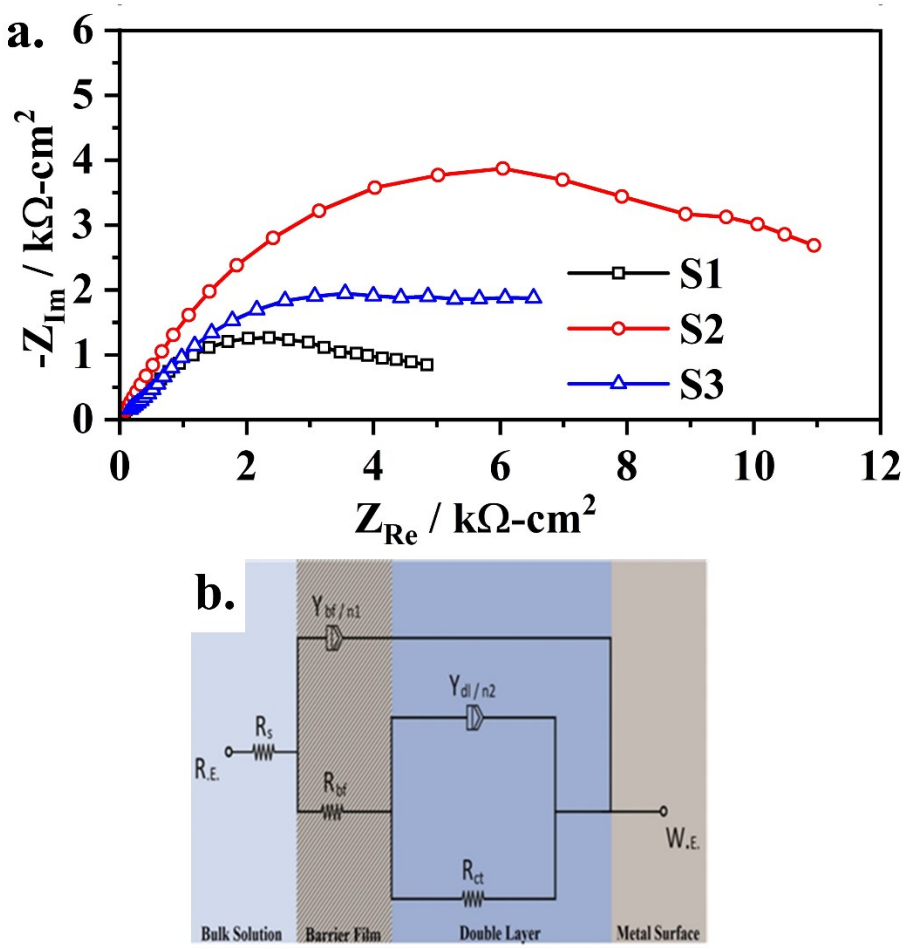

Figure 1: Electrochemical impedance spectroscopy of SS304 samples exposed to (a) Nyquist plots obtained in S1, S2, and S3 media at a constant temperature of 37 °C after 14 days of incubation.

(b) EEC model used to simulate impedance spectra for quantification of electrochemical parameters.

Table 4: Quantitative values of electrochemical parameters obtained by simulating the impedance spectra with an EEC model (as shown in Figure 1b)

Systems	R_s ($\Omega.cm^2$)	Y_{bf} (mSs^{n_1}/cm^2)	n_1	R_{bf} ($k\Omega.cm^2$)	Y_{dl} (mSs^{n_2}/cm^2)	n_2	R_{ct} ($k\Omega.cm^2$)
S1	22.03	79.17	0.92	3.22*	1.18	0.77	4.85
S2	8.98	25.83	0.46	6.04	37.23	0.53	11.14
S3	20.44	51.44	0.71	4.00	53.39	0.76	6.53

*Precipitation of the salt in MSM medium on the surface of SS304 sample by forming a salt layer

The Tafel polarization curves of the SS304 samples were also obtained in S1, S2 and S3 media as shown in **Figure 2**. These polarization curves were extrapolated to obtain Tafel slopes (β_a, β_c), corrosion current (i_{corr}) and corrosion potential (E_{corr}) as given in Table 5. The i_{corr} values of SS304 samples are related to the corrosion rate as calculated by using Faradays' law.

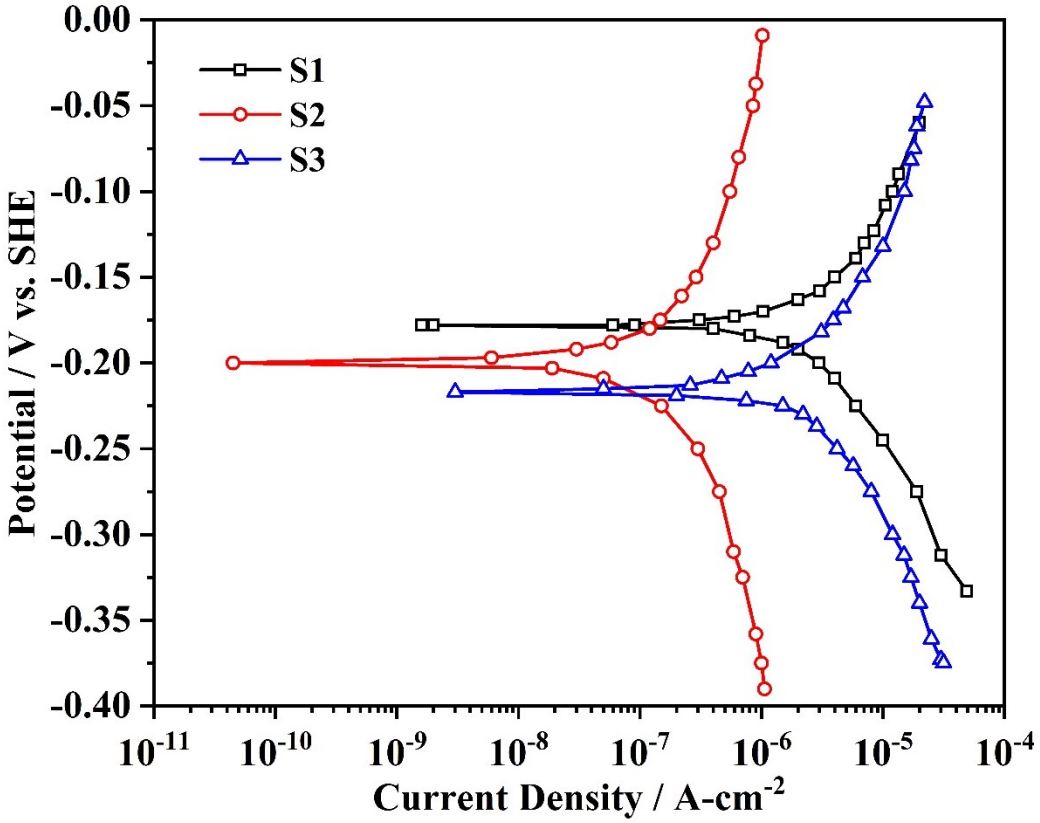

Figure 2: Potentiodynamic polarization scans to determine corrosion kinetic parameters of SS304 in S1, S2, and S3 media. (**Note:** These tests were conducted at a constant temperature of 37 ^{0}C and after 14 days of incubation in these media)

Table 5: Values of corrosion related parameters

Parameters	S1	S2	S3
Corrosion potential (E_{corr}; mV vs. Ag/AgCl)	-178	-199	-212
Corrosion current (i_{corr}; μA/cm^2)	2.67	0.13	2.14
Tafel slope for anodic curve (β_a; mV/decade)	89	115	89
Tafel slope for cathodic curve (β_c; mV/decade)	152	200	175
Corrosion rate (μm year^{-1})	34.91	1.69	28.02

The microscopic features of the SS304 sample surface exposed to S2 and S3 media at 37 C after 14 days of incubation as shown in **Figure 3**. The biofilms were fixed on the surface by immersing in 3% glutaraldehyde. The SEM images showed the presence of rod-shaped bacteria encapsulated in EPS matrix and a formed thick and adherent biofilm of PA-ZK strains (**Figure 3a**). In the case of BS-S1X strain, threads like a 3D network of biofilm were formed on the surface of the SS304 sample as shown in **Figure 3b**. The biofilms were removed by immersing the exposed samples in 1 M HNO_3 solution. Compared to the as-prepared SS304 sample (ground surface up to 1200 grit size), appreciable surface dissolution was observed after exposure to S1 as shown in **Figures 4a and 4b**. Also, after cleaning, the samples exposed to S2 presented a relatively smooth surface compared to the sample exposed to the S3 systems, which experience pitting as shown in **Figures 4c and 4d**.

The FTIR spectra of both PA-ZK and BS-S1X bacterial strains SS304 surface were obtained as shown in **Figure 5**. The reflectance signatures originated at 400-900 cm^{-1} were associated with the presence of *metal oxides* i.e. Fe, Ni, Cr oxides that can be expected due to the release of metallic ions from the surface of SS304 samples. The presence of alcoholic and ether groups was evident from the appearance of peaks at 900-1,400 cm^{-1}. The peaks observed at ~1,550 cm^{-1} and ~1,650 cm^{-1} corresponded to the amide II and amide I groups, respectively. Carboxylic acid and NH/OH functional groups were represented by the peaks observed at 2,400 cm^{-1} and 3,400-3,900 cm^{-1}, respectively. The origin of these peaks was associated with the organic species in the EPS (in the biofilm) that could remain on the surface of SS304 after exposure to bacterial strains even after surface cleaning.

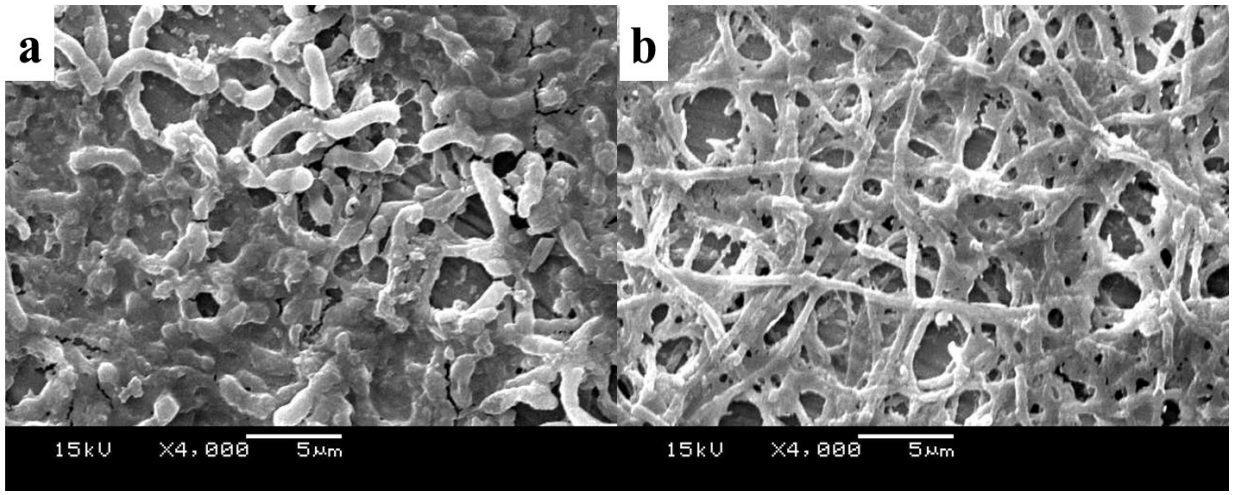

Figure 3: SEM images of SS304 having (a) *P. aeruginosa* ZK strain and (b) *B. subtilis* S1X strain biofilms after 14 days of incubation at 37 °C and treated with 3% glutaraldehyde

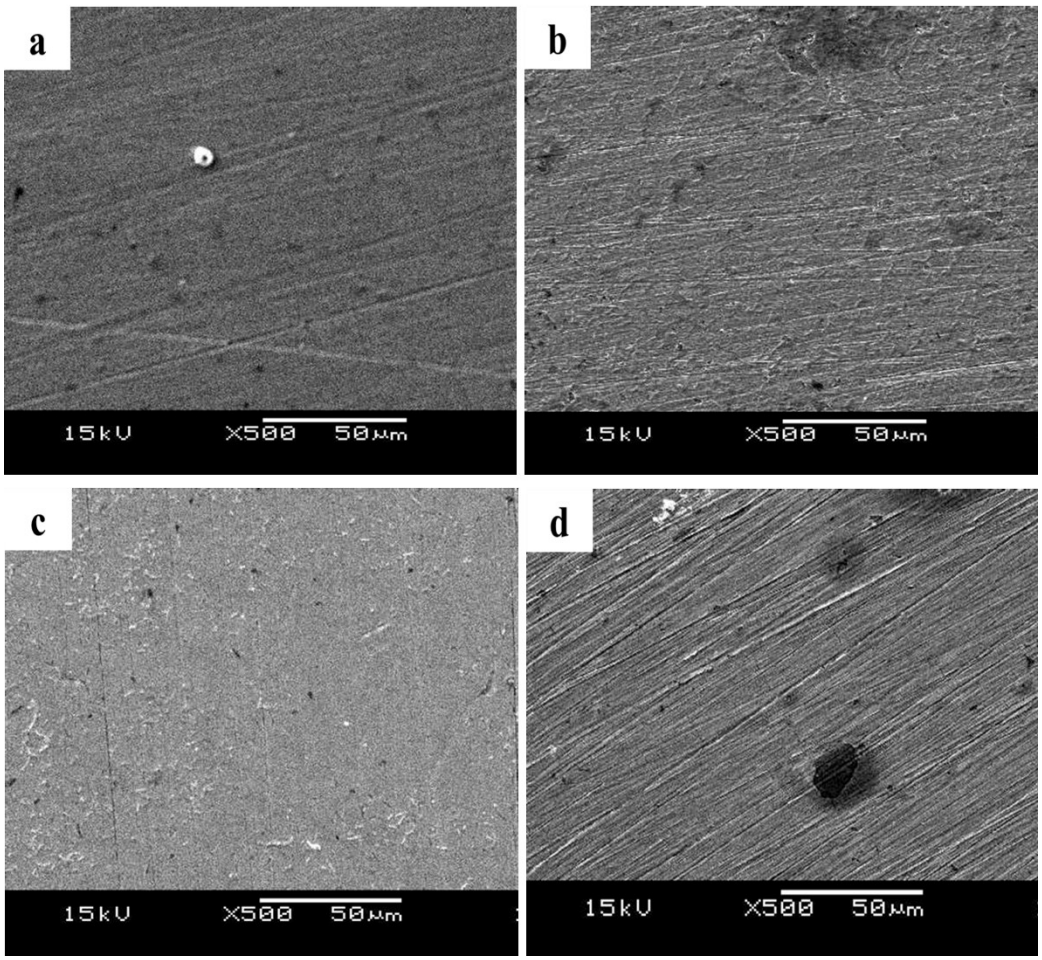

Figure 4: Surface morphology of SS304 samples after cleaning and removal of biofilm by immersion in 1 M HNO_3 solution (a) as-prepared and cleaned SS304 without exposure to bacterial strains, and samples (b) exposed to S1, (c) S2, and (d) S3 media.

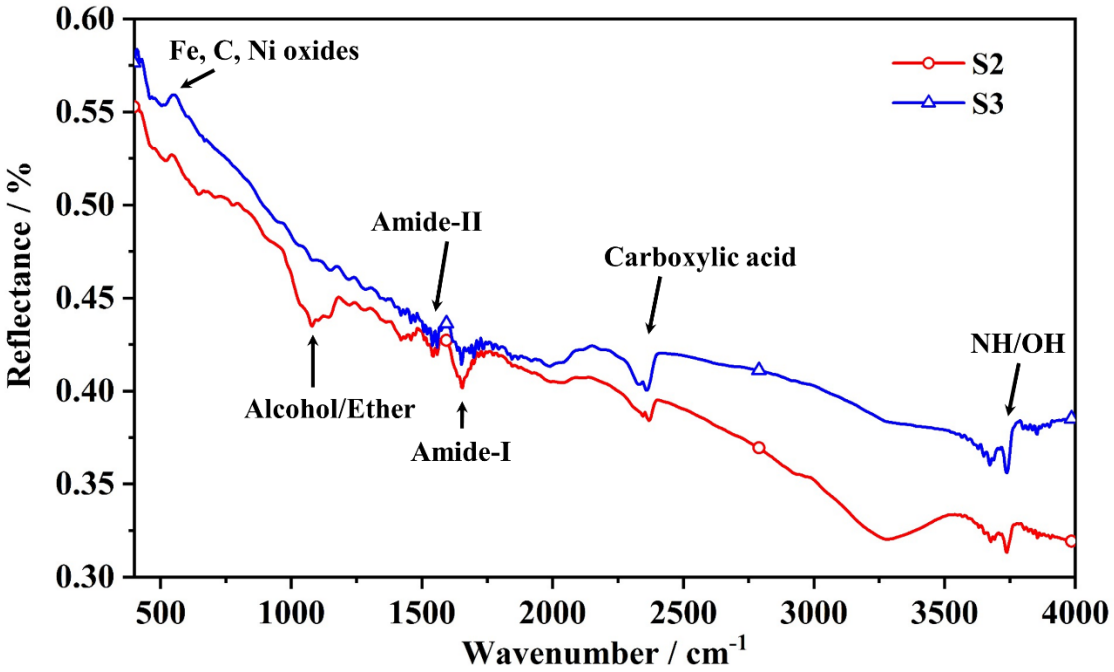

Figure 5: FTIR spectra of the EPS produced on the surface of SS304 by *P. aeruginosa* strain ZK and *B. subtilis* strain S1X containing biofilms

4. Discussion

The biocorrosion is a great challenge and posed detrimental effects on the mechanical integrity of the metallic structures. In this work, the corrosion behavior of SS304 has been investigated in the presence of two bacteria strains i.e., PA-ZK and BS-S1X strains. Both bacterial strains were found to be hydrophobic as evaluated from the BATH and SAT. The degree of hydrophobicity is linked with the stability of the biofilm and proliferation of the bacteria on the surface of SS304. In other words, the presence of biofilm and bioactivity of the bacteria could affect the surface energy of the metal and may alter its hydrophobic character. The macromolecules i.e., lipids, polysaccharides, nucleic acids etc present in the extracellular polymeric substance (EPS) could interact with the dissolved metal ions and control the MIC. However, the stability of a biofilm and its interaction with the surface strongly depends on the nature of the EPS, and chemical composition, topography, and microstructural features of the alloy [21, 22]. After exposure to bacterial strains, the improved degree of hydrophobicity (~35%) corresponded to the barrier characteristics of the biofilms, which could be beneficial to reduce aqueous corrosion. For instance, the hydrophobic character is related to the barrier characteristics of the biofilm, which is validated by the limited ingress of aggressive ionic species at the biofilm/substrate interface. The barrier characteristics of the biofilm were

evident in the impedance spectra (Figure 1). The results reported in Table 4 highlighted the relatively large resistance of the biofilm (R_{bf}) compared to the resistance of the MSM layer that could form on the surface of SS304 in the controlled medium. Similarly, improved corrosion resistance (as indicated by R_{ct} values) was directly associated with the limited transport of the ionic species through the biofilm and interaction with the substrate [20, 23, 24]. These R_{bf} and R_{ct} values were obtained after fitting the impedance spectra by iterating the input values of each parameter in the EEC model with the help of Echem Analyst software (Gamry®). The results corroborated the interfacial electrochemical processes at the surface of the SS304 sample and barrier properties of the biofilm. For instance, in the S1 medium, the species i.e. glucose, amino acids and salts in the MSM could precipitate and deposit on the SS304 surface. These deposited species could form a defective surface layer through which electrolytes could penetrate and reach the substrate causing corrosion. Comparatively small values of R_{bf} (3.22 kΩ-cm^2) and R_{ct} (4.85 kΩ-cm^2) exhibited by the SS304 sample in the S1 medium validated its poor corrosion resistance. On the other hand, in the inoculated media (i.e., S2 and S3), the relatively large values of R_{bf} and R_{ct} were registered by the SS304 samples. For instance, the SS304 sample in the S2 medium registered relatively large values of Rbf (6.04 kΩ.cm^2) and R_{ct} (11.14 kΩ.cm^2) compared to the low R_{bf} and R_{ct} values of the SS304 sample in S3 medium (4.00 and 6.53 kΩ.cm^2, respectively) as given in Table 4. These small values were attributed to the defective structure of the biofilm that was formed on the surface of SS304 by the BS-S1X bacteria strain. In simple words, the porous or defective structure of the biofilm could facilitate the ingress of ionic species to the biofilm/substrate interface. On the other hand, the formation of relatively compact and adherent PA-ZK bacteria containing biofilm (in S2 medium) hindered the penetration of electrolyte and restricted the progress of corrosion reactions at the biofilm/substrate interface as evident from the large R_{bf} and R_{ct} values [15, 25, 26]. The ingress of ionic species at the biofilm/substrate interface and defective structure of biofilm was further confirmed from the increased charge relaxation in the double layer that could form within the porous structure of the biofilm. This was evident from the relatively large Y_{dl} (53.39 mS^{n2}/cm^2) and Y_{bf} (51.44 mS^{n1}/cm^2) values as registered by the SS304 samples in the S3 compared to the corresponding values in the S2 medium as given in Table 4 [15]. In other words, the larger values of $_{Ydl}$ are directly related to the porous structure of the biofilm and exposed surface area of the SS304 sample to the aggressive ionic species in the inoculated medium.

The kinetic of corrosion processes was evaluated from the Tafel polarization curves and the quantitative information is given in Table 5. The poor corrosion resistance of the SS304 sample in the S1 medium is evaluated from the large i_{corr} (2.67 μA/cm^2) and the corresponding corrosion rate of 34.91 μm-year^{-1}. However, appreciably small i_{corr} (0.13 μA/cm^2) of the SS304 sample in S2 medium validated the corrosion inhibitive effects of the PA-ZK biofilm. On the other hand, a large corrosion rate (28.02 μm-year^{-1}) of the SS304 in the S3 medium validated the poor barrier characteristics of the BS-S1X biofilm. The inhibitive action of the biofilm can be estimated by comparing the Tafel slope values (β_a and β_c). For instance, the large β_a and β_c (0.15 and 0.2 V/decade, respectively) values of the SS304 in the S2 medium were attributed to barrier characteristics of the biofilm. On the other hand, comparatively small β_a and β_c values were registered by the SS304 sample in S1 and S3 media. This corresponded to the progress of localized reactions within the porous structure of the film as evident from the presence of pits on the surface of the SS304 (Figures 4b and 4d). The presence of surface layer (in case of the S1 medium) and biofilms (in the case of S2 and S3 media) could preferentially cover the cathodic regions on the SS304 sample and may impede the corrosion process as confirmed from the relatively large β_c values compared to β_a. However, the formation of a non-homogeneous surface layer in the S1 medium and the presence of porous structure of the biofilm in the S3 medium facilitated the localized corrosion reactions. However, the limited approach of the ionic species through the compact biofilm produced by PA-ZK bacteria in the S2 medium controlled the dissolution of the SS304. This behavior can also be validated from the impedance data (Table 4) and the results are well in agreement with the characteristics of the biofilms as explained above. A noticeable shift in E_{corr} to more negative values and relatively large β_c values of SS304 in S2 and S3 media compared to S1 medium represented the restricted oxygen reduction reaction owing to the nature of the EPS in the biofilm [27].

Figure 3 shows the formation of thick and uniform EPS in which the rod-shaped bacteria were well distributed. This biofilm was produced by the biological activity and proliferation of the PA-ZK bacteria on the surface of SS304 during 14 days of incubation. Due to the biological activities of the bacteria in the dense biofilm, in the produced EPS layer, the dissolved oxygen within this biofilm is consumed and introduced a concentration gradient as shown in Figure 6. The depletion of the dissolved oxygen at the biofilm/substrate interface could result in surface polarization and limited the corrosion reactions controlled by the supply of oxygen at the SS304 surface. In the

presence of dense and uniform PA-ZK containing biofilm, the dissolved oxygen was consumed by the biological activities of the bacteria and SS304 and limited current in cathodic polarization curve of S2 system (Figure 2) was attributed to the depletion of oxygen. However, the biofilm produced by *BS*- S1X bacteria contained pores and the SS304 surface was locally exposed to the ionic species in the S3 medium. The localized dissolution of the SS304 was associated with the formation of differential aeration cells within the porous EPS containing biofilm. These effects were evident after the removal of biofilm, where the topographical analysis revealed localized corrosion of the SS304 samples in both S1 and S3 media. Due to the dissolution of the metal ions at the local anodic sites, the EPS layer is modified and facilitates electron tunnelling, which may result in an increased corrosion rate due to the depolarization of the cathodic regions. The origin of reflectance peaks in the FTIR spectra within 400 and 900 cm^{-1} confirmed the stretching vibrations of the Fe, Cr and Ni oxides in the EPS layer. Similarly, the peaks signatures between (900 – 1400 cm^{-1}), 1550 and at 1650 cm^{-1}) corresponded to the ether (C-O-C), amide I and amide II functional groups, which represent the presence of polysaccharide and protein molecules on the surface of SS304 samples. The peak between 3400 to 3900 cm^{-1} (NH/OH) were attributed to the hydroxyl group of the adsorbed water and amino group (NH) of proteins in the EPS [28-31].

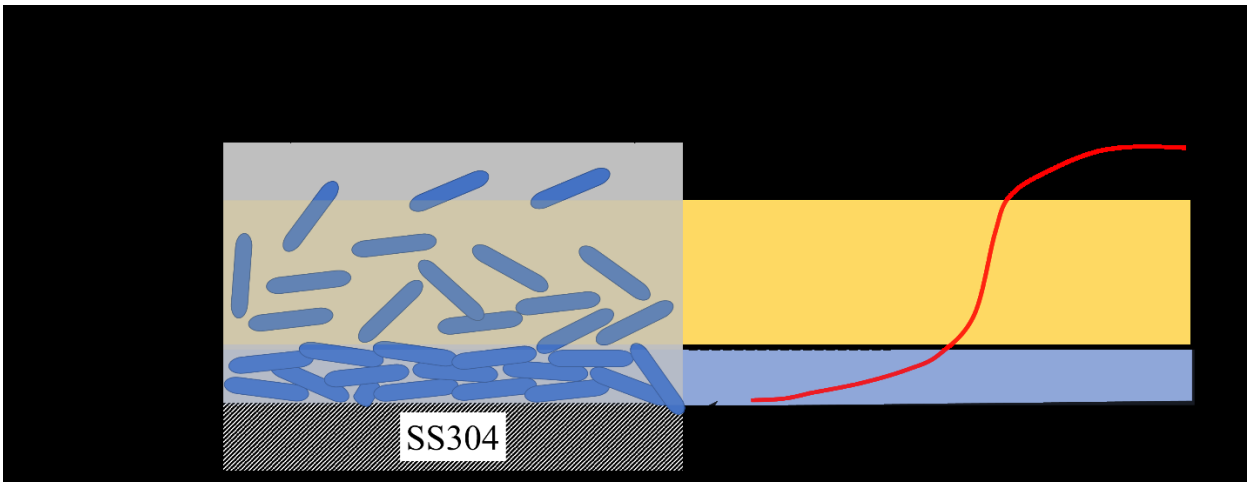

Figure 6: (a) Schematic of biofilm formation showing the presence of bacteria in the EPS (b) Hypothetical representation of O_2 concentration variation in the biofilm

Conclusions

This research work focuses on the corrosion behavior of SS304 in the presence of the PA-ZK and BS-S1X bacterial strains incubated for 14 days at 37 °C. The morphology and electrochemical behavior of the biofilms formed by these bacterial strains were found to be different. For instance,

the biofilm produced by the PA-ZK strain was denser and uniform compared to the biofilm produced by BS-S1X bacteria. In the case of PA-ZK, the presence of a dense EPS layer retarded the corrosion rate of SS304 compared to the porous structure of the EPS layer formed by BS-S1X bacteria. The increased hydrophobicity of the biofilm produced by these bacterial strains was evident from the BATH and salt aggregation tests. However, the formation of a non-homogeneous EPS layer by BS-S1X bacteria facilitated the ingress of ionic species through the biofilm. The defective structure of this biofilm resulted in a significantly large corrosion rate (28.02 μm/yr) of the substrate (SS304) compared to 1.69 μm/yr as registered by PA-ZK-containing film. The inferior barrier characteristics of the biofilm produced by BS-S1X were also confirmed from the small R_{bf} and 'R_{ct}' (4.0 and 6.53 kΩ-cm^2, respectively) values. These values were comparable to the R_{bf} and R_{ct} values of the SS304 in the controlled medium indicating the ineffectiveness of the BS-S1X containing biofilm towards corrosion inhibition as evaluated from the impedance spectra. On the other hand, a large β_c (0.2 V/decade) and R_{ct} (11.14 kΩ-cm^2) registered by the PA-ZK containing biofilm validated the decrease in corrosion of SS304, specifically controlled by the cathodic polarization. In other words, the dense EPS layer produced by the PA-ZK bacteria inhibited corrosion of the SS304 by restricting the reduction of dissolved oxygen or other oxidants indicating the barrier characteristics of the biofilm.

References

1. Videla HA, Herrera LK: **Microbiologically influenced corrosion: looking to the future**. *International microbiology* 2005, **8**(3):169-180.
2. Qu Q, He Y, Wang L, Xu H, Li L, Chen Y, Ding Z: **Corrosion behavior of cold rolled steel in artificial seawater in the presence of *Bacillus subtilis* C2**. *Corrosion Science* 2015, **91**:321-329.
3. Reza J: **Microbiologically influenced corrosion: An Engineering Insight**, 2nd edn: Springer International Publishing; 2017.
4. Liu H, Gu T, Zhang G, Wang W, Dong S, Cheng Y, Liu H: **Corrosion inhibition of carbon steel in CO2-containing oilfield produced water in the presence of iron-oxidizing bacteria and inhibitors**. *Corrosion Science* 2016, **105**:149-160.
5. Jia R, Yang D, Xu D, Gu T: **Mitigation of a nitrate reducing *Pseudomonas aeruginosa* biofilm and anaerobic biocorrosion using ciprofloxacin enhanced by D-tyrosine**. *Scientific Reports* 2017, **7**(1):1-11.

6. Soltani N, Tavakkoli N, Kashani MK, Mosavizadeh A, Oguzie E, Jalali M: ***Silybum marianum*** **extract as a natural source inhibitor for 304 stainless steel corrosion in 1.0 M HCl**. *Journal of Industrial and Engineering Chemistry* 2014, **20**(5):3217-3227.
7. Nagiub A, Mansfeld F: **Evaluation of microbiologically influenced corrosion inhibition (MICI) with EIS and ENA**. *Electrochimica Acta* 2002, **47**(13-14):2319-2333.
8. Gunasekaran G, Chongdar S, Gaonkar S, Kumar P: **Influence of bacteria on film formation inhibiting corrosion**. *Corrosion Science* 2004, **46**(8):1953-1967.
9. San NO, Nazır H, Dönmez G: **Microbially influenced corrosion and inhibition of nickel–zinc and nickel–copper coatings by *Pseudomonas aeruginosa***. *Corrosion Science* 2014, **79**:177-183.
10. Liu H, Gu T, Asif M, Zhang G, Liu H: **The corrosion behavior and mechanism of carbon steel induced by extracellular polymeric substances of iron-oxidizing bacteria**. *Corrosion Science* 2017, **114**:102-111.
11. Batmanghelich F, Li L, Seo Y: **Influence of multispecies biofilms of *Pseudomonas aeruginosa* and *Desulfovibrio vulgaris* on the corrosion of cast iron**. *Corrosion Science* 2017, **121**:94-104.
12. Xu D, Li Y, Gu T: **Mechanistic modeling of biocorrosion caused by biofilms of sulfate reducing bacteria and acid producing bacteria**. *Bioelectrochemistry* 2016, **110**:52-58.
13. Li S, Li L, Qu Q, Kang Y, Zhu B, Yu D, Huang R: **Extracellular electron transfer of *Bacillus cereus* biofilm and its effect on the corrosion behaviour of 316L stainless steel**. *Colloids and Surfaces B: Biointerfaces* 2019, **173**:139-147.
14. Videla HA, Herrera LK: **Understanding microbial inhibition of corrosion. A comprehensive overview**. *International Biodeterioration & Biodegradation* 2009, **63**(7):896-900.
15. Zhang D, Qian H, Xiao K, Zhou F, Liu Z, Li X: **Corrosion inhibition of 304 stainless steel by *Paecilomyces variotii* and *Aspergillus niger* in aqueous environment**. *Corrosion Engineering, Science and Technology* 2016, **51**(4):285-290.
16. Wadood HZ, Sabri AN: **Screening, characterization and biofilm formation of nickel resistant bacteria isolated from indigenous environment**. *Pol J Microbiol* 2013, **62**:411-418.

17. Wadood HZ, Rajasekar A, Ting YP, Sabari AN: **Role of *Bacillus subtilis* and *Pseudomonas aeruginosa* on corrosion behaviour of stainless steel**. *Arabian Journal for Science and Engineering* 2015, **40**(7):1825-1836.
18. Rosenberg M: **Bacterial adherence to hydrocarbons: a useful technique for studying cell surface hydrophobicity**. *FEMS Microbiology Letters* 1984, **22**(3):289-295.
19. Basson A, Flemming L, Chenia H: **Evaluation of adherence, hydrophobicity, aggregation, and biofilm development of *Flavobacterium johnsoniae*-like isolates**. *Microbial ecology* 2008, **55**(1):1-14.
20. Wadood HZ, Rajasekar A, Farooq A, Ting YP, Sabri AN: **Biocorrosion inhibition of Cu70: Ni30 by Bacillus subtilis strain S1X and Pseudomonas aeruginosa strain ZK biofilms**. *Journal of Basic Microbiology* 2020, **60**(3):243-252.
21. Krasowska A, Sigler K: **How microorganisms use hydrophobicity and what does this mean for human needs?** *Frontiers in cellular and infection microbiology* 2014, **4**:112.
22. Mirani ZA, Fatima A, Urooj S, Aziz M, Khan MN, Abbas T: **Relationship of cell surface hydrophobicity with biofilm formation and growth rate: A study on Pseudomonas aeruginosa, Staphylococcus aureus, and Escherichia coli**. *Iranian Journal of Basic Medical Sciences* 2018, **21**(7):760.
23. Lodhi M, Deen K, Rahman ZU, Farooq A, Haider W: **Electrochemical characterization and thermodynamic tendency of β-Lactoglobulin adsorption on 3D printed stainless steel**. *Journal of Industrial and Engineering Chemistry* 2018, **65**:180-187.
24. Chen S, Zhang D: **Study of corrosion behavior of copper in 3.5 wt.% NaCl solution containing extracellular polymeric substances of an aerotolerant sulphate-reducing bacteria**. *Corrosion Science* 2018, **136**:275-284.
25. Lekbach Y, Li Z, Xu D, El Abed S, Dong Y, Liu D, Gu T, Koraichi SI, Yang K, Wang F: ***Salvia officinalis* extract mitigates the microbiologically influenced corrosion of 304L stainless steel by *Pseudomonas aeruginosa* biofilm**. *Bioelectrochemistry* 2019, **128**:193-203.
26. Zhou E, Li H, Yang C, Wang J, Xu D, Zhang D, Gu T: **Accelerated corrosion of 2304 duplex stainless steel by marine *Pseudomonas aeruginosa* biofilm**. *International Biodeterioration & Biodegradation* 2018, **127**:1-9.

27. K. M. Deen, M. Yousaf, N. Afzal, S. Riaz, S. Naseem, A. Farooq, I. M. Ghauri, Microbiological influenced corrosion attack by the Bacillus Megaterium bacteria on Al-Cu alloy, *Materials Technology: Advanced Performance Materials*, 2014, **29(5)**, 269-275.
28. Rajasekar A, Ting Y-P: **Microbial corrosion of aluminum 2024 aeronautical alloy by hydrocarbon degrading bacteria *Bacillus cereus* ACE4 and *Serratia marcescens* ACE2**. *Industrial & engineering chemistry research* 2010, **49**(13):6054-6061.
29. Guo Z, Liu T, Cheng YF, Guo N, Yin Y: **Adhesion of *Bacillus subtilis* and *Pseudoalteromonas lipolytica* to steel in a seawater environment and their effects on corrosion**. *Colloids and Surfaces B: Biointerfaces* 2017, **157**:157-165.
30. Naik UC, Srivastava S, Thakur IS: **Isolation and characterization of *Bacillus cereus* IST105 from electroplating effluent for detoxification of hexavalent chromium**. *Environmental Science and Pollution Research* 2012, **19**(7):3005-3014.
31. Dutta A, Bhattacharyya S, Kundu A, Dutta D, Das AK: **Macroscopic amyloid fiber formation by *staphylococcal* biofilm associated SuhB protein**. *Biophysical chemistry* 2016, **217**:32-41.